Progress In Electromagnetics Research M, Vol. 13, 95–108, 2010

SAR AND TEMPERATURE ELEVATION IN A MULTI-LAYERED HUMAN HEAD MODEL DUE TO AN OBLIQUELY INCIDENT PLANE WAVE

A. I. Sabbah and N. I. Dib

Electrical Engineering Department
Jordan University of Science & Technology
Irbid, Jordan

M. A. Al-Nimr

Mechanical Engineering Department
Jordan University of Science & Technology
Irbid, Jordan

Abstract—In this paper, the Specific Absorption Rate (SAR) distribution in a human head irradiated by an obliquely incident electromagnetic plane wave is studied. A simple planar multi-layered structure is used to model the human head. Moreover, the steady state thermal elevation distribution is calculated by solving the bioheat equation using the finite difference time domain (FDTD) method. Both types of wave polarization (perpendicular and parallel) will be discussed. The obtained results confirm the importance of performing a thermal analysis along with the dosimetric one. It is found that the induced temperature elevation in the brain region, in all the examined conditions, never exceeds 0.4°C. This value is well below the threshold for the induction of adverse thermal effects to the neurons which is 3.5°C.

1. INTRODUCTION

Due to the rapid increase in using the cellular phones and WLANs, concerns regarding potential health hazards due to the absorption of Electromagnetic (EM) waves have been growing. International organizations (such as the American National Standard Institution/Institution of Electrical and Electronic Engineering (ANSI/IEEE) and the International Commission on Non-Ionizing

Corresponding author: A. I. Sabbah (asabbah84@gmail.com).

Radiation Protection (ICNIRP)) have put limits on the maximum Specific Absorption Rate (SAR), which has been widely used to determine the possibility of health hazards in the human head due to Radio Frequency (RF) radiation [1, 2]. These limits are mainly based on the findings from experiments on animals.

Because of the fact that the biological hazards are mainly due to temperature rise in the tissue, the safety guidelines on localized SAR for wireless applications should be determined in relation to temperature rise in the head. Although temperature elevation is an important parameter, little is known about it.

In the literature, Riu and Foster [3] considered a semi-infinite homogeneous plane of tissue. A 3-layerd sphere model that represents skin, bone and brain was considered by Khalatbari et al. [4]. An inhomogeneous human head model with 32 tissues has been used in [5]. Two problems are faced in these models; first, the rather long execution time needed in order to get the results; in the best case it requires few hours using an ordinary PC. The second problem is that the cell size used in these models is considered a low resolution for head models, and thus, the effect of thin layers such as skin, fat and Dura is usually not fully evaluated.

In this paper, a simple planar multi-layered human head model will be used to calculate the electric field and SAR distributions inside the head when exposed to an obliquely incident plane wave. The temperature rise in the human head for wireless applications will be also computed using the finite difference time domain (FDTD) method.

2. NUMERICAL METHOD AND MODELING

Since the number of existing anatomical computer models is small, and their resolution is often not sufficient to study the effects of tissues with small thicknesses, a simple planar multi-layered head model is used here. This head model was originally proposed by Akram and Andrew in [6], and it consists of skin, fat, bone, Dura, CSF and brain as shown in Figure 1. The mobile phone antenna (or WLAN antenna) exists in air at a specific distance from the head model. It is assumed that this antenna produces a uniform plane wave that is obliquely incident on the multi-layer planar structure.

This model is chosen because it does not need extensive numerical techniques for SAR and temperature elevation calculations. In addition, it will be demonstrated that this rather simple model will produce SAR values that are very close to those obtained using other more elaborate models. The effect of thin layers will be figured out precisely. Up to our knowledge, this model has not been used before

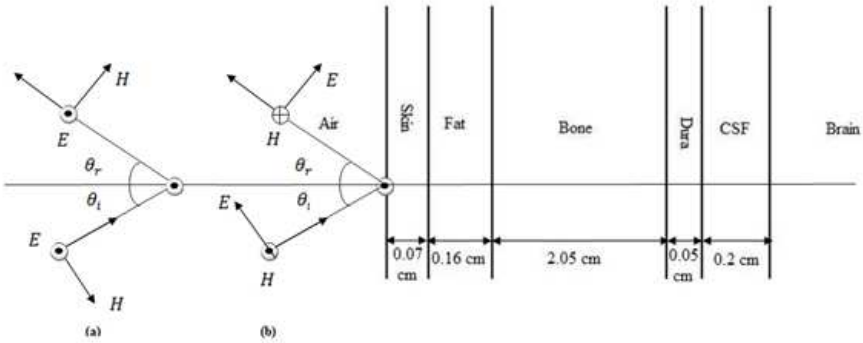

Figure 1. The six-layer planar human head model used in this paper with an obliquely incident plane wave of (a) perpendicular polarization, or (b) parallel polarization.

Table 1. Relative permittivity and conductivity of the layers of the human head model [7].

Layer	Relative permittivity			Conductivity (S/m)		
	900 MHz	1800 MHz	2.4 GHz	900 MHz	1800 MHz	2.4 GHz
Skin	41.4	38.9	38.1	0.87	1.18	1.44
Fat	5.46	5.34	5.29	0.051	0.078	0.102
Bone	12.45	11.8	11.41	0.14	0.28	0.385
Dura	44.4	42.9	42.1	0.96	1.32	1.64
CSF	68.7	67.2	66.3	2.41	2.92	3.41
Brain	45.8	43.5	42.6	0.77	1.15	1.48

to find out temperature elevation in the head exposed to an obliquely incident plane wave.

The electrical properties of human tissues control the propagation, reflection, attenuation, and other properties of EM fields in the body. These properties depend strongly on the tissue type and the frequency of interest. As the water content in the tissue increases, the conductivity increases. Table 1 shows the electrical properties of the different tissues in the head model at 900, 1800 and 2400 MHz [7]. These frequency bands are commonly used in cellular phones and WLANs. It should be noted that the averaged values between white and grey brain tissues are used as the electrical properties of brain. It is also worth mentioning that the body is so weakly magnetic such that, generally, the relative permeability μ_r can be assumed to be 1 [8].

The unknown incident and reflected field amplitudes in each layer

can be found by applying the appropriate boundary conditions at the interfaces. Specifically, enforcing the continuity of the tangential components of $\vec{E}$ and $\vec{H}$ at the interfaces leads to a set of twelve equations [9]. Solving this set of equations yields the amplitudes of the incident and reflected electric fields at the interfaces. The total electric field in the ith layer can be calculated using the following equation:

$$\vec{E}_{t_i} = \vec{E}_{i_i} + \vec{E}_{r_i} \tag{1}$$

Matlab codes were implemented using the approach presented in [9] to calculate the electric field distribution in all layers of the head model. For practical considerations, (and assuming the worst case) the total power radiated by the cellular phone (or WLAN) antenna is assumed to be 0.6 W, and the distance between the head and the phone is assumed to be 2 cm. From this data, the electric field in the air (E_{fo}) is calculated and found to be 300 V/m. The SAR (W/kg) is calculated by the following equation:

$$\mathrm{SAR}_i = \frac{\sigma_i |E_i|^2}{2\rho_i} \tag{2}$$

where σ_i, $|E_i|$ and ρ_i are the ith tissue conductivity, total electric field, and density, respectively. The values of ρ_i for the different tissues of the model are taken from [10] and are given in Table 2.

Tissue temperature distributions during exposure to RF waves can be determined by solving the bioheat transfer equation (BHE), which considers the contributions of heat conduction, blood perfusion, and external heating. Blood perfusion rate is defined as the amount of blood supplied to a certain tissue region per minute per 100 g tissue weight.

In addition to the geometrical parameters and thermal properties, SAR distribution induced by the external heating device should be determined first. Pennes [11] proposed a mathematical model to describe the effects of metabolism and blood perfusion on the energy balance within the tissue. It was written in the following form:

$$C_p(z)\rho(z)\frac{\partial T(z,t)}{\partial t} = K(z)\nabla^2 T(z,t) + \rho(z)\mathrm{SAR}(z) - B(z)(T(z,t) - T_b) \tag{3}$$

Table 2. Tissues density of the layers of the human head model [10].

Tissue	Skin	Fat	Bone	Dura	CSF	Brain
ρ (kg/m^3)	1100	920	1850	1050	1060	1030

where T is the temperature of the tissue, T_b is the temperature of the blood, K is the thermal conductivity of the tissue, C_p is the specific heat of the tissue, and B is a term associated with blood perfusion.

The temperature elevation due to handset antennas can be considered as sufficiently small not to activate the thermoregulatory response; including the increase of local blood flow and the activation of sweating mechanism. Thus, this response is neglected in the present study. Next, a boundary condition is needed to account for the heat exchange between the head surface; namely, the skin, and the external environment. It is given as follows:

$$K(z_{\min})\frac{\partial T(z,t)}{\partial z} = -h(T(z_{\min},t) - T_a) \tag{4}$$

where h, T, and T_a denote, respectively, the heat transfer coefficient, the surface temperature of the tissue, and the temperature of the air. The thermal parameters used in this study are given in Table 3 [12]. The convective heat transfer coefficient between the model surface and air (h) is set to $10.5\,\mathrm{W/(^\circ C\ m^2)}$, which is the typical value of the free convection mode of air at room temperature. The ambient temperature (T_a) and the blood temperature (T_b) are set to 20°C and 37°C, respectively.

By expanding the BHE in its finite difference approximation, (3) and (4) can be written as follows:

$$\begin{aligned} T^{m+1}(i) &= T^m(i) + \frac{\Delta t}{C_p(i)}SAR(i) - \frac{\Delta t B(i)}{C_p(i)\rho(i)}(T^m(i) - T_b) \\ &\quad + \frac{\Delta t K(i)}{C_p(i)\rho(i)\Delta z^2}[T^m(i+1) + T^m(i-1) - 2T^m(i)] \end{aligned} \tag{5}$$

$$T^{m+1}(i_{\min}) = \frac{K(i_{\min})T^m(i_{\min}+1)}{K(i_{\min}) + h\Delta z} + \frac{T_a h\Delta z}{K(i_{\min}) + h\Delta z} \tag{6}$$

Table 3. Thermal parameters of head tissues [12].

Tissue	K W/(K·m)	C_p J/(K·kg)	B W/(K·m^3)
Skin	0.42	3600	9100
Fat	0.25	3000	1700
Bone	0.39	3100	1850
Dura	0.5	3600	1125
CSF	0.62	4000	0
Brain	0.535	3650	40000

The temperature rise due to the RF exposure is obtained from the difference between the temperature $T(z,t)$ and $T(z,0)$, where $T(z,0)$ is the normal temperature distribution in the unexposed head, i.e., with $SAR = 0$ at thermal equilibrium. A stability criterion is needed in order to make sure that the heat transfer distribution is true. The numerical stability condition for the time step used in solving the BHE in its finite-difference form can be derived by expressing the solution using the Fourier series and by checking the variation of amplitude of each Fourier component. In order to ensure the numerical stability, Δt is chosen to satisfy:

$$\Delta t \leq \frac{2C_p \rho \Delta z^2}{12K + B\Delta z^2} \tag{7}$$

which is derived from Von Neumann's condition [13]. A cell resolution of 0.1 mm is used in Equations (5)–(7).

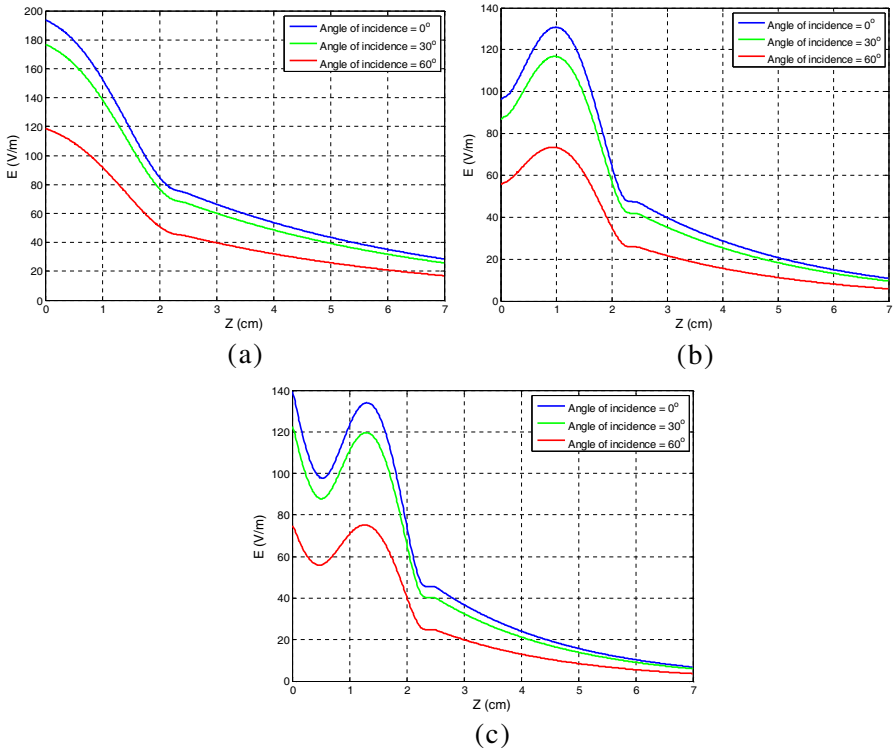

Figure 2. Induced total electric field intensity in the head model for perpendicular polarization ($E_{fo} = 300\,\mathrm{V/m}$) at (a) 900 MHz, (b) 1800 MHz, (c) 2.4 GHz.

3. RESULTS

The total electric field intensity in each layer of the multi-layered model has been calculated at different incidence angles $(0°, 30°, 60°)$ and is shown in Figures 2 and 3 at frequencies of 900 MHz, 1800 MHz and 2.4 GHz for perpendicular and parallel polarizations, respectively. These figures show that for the same incidence angle, the electric field inside the human head in the case of parallel polarization is larger than that in the case of perpendicular polarization. This may be due to a higher field reflection by the skin layer in the perpendicular polarization case as compared to the parallel polarization case [9].

It is worth mentioning that the electric field in perpendicular polarization has one component only which is tangential to the interface. Thus, the electric field must be continuous across the

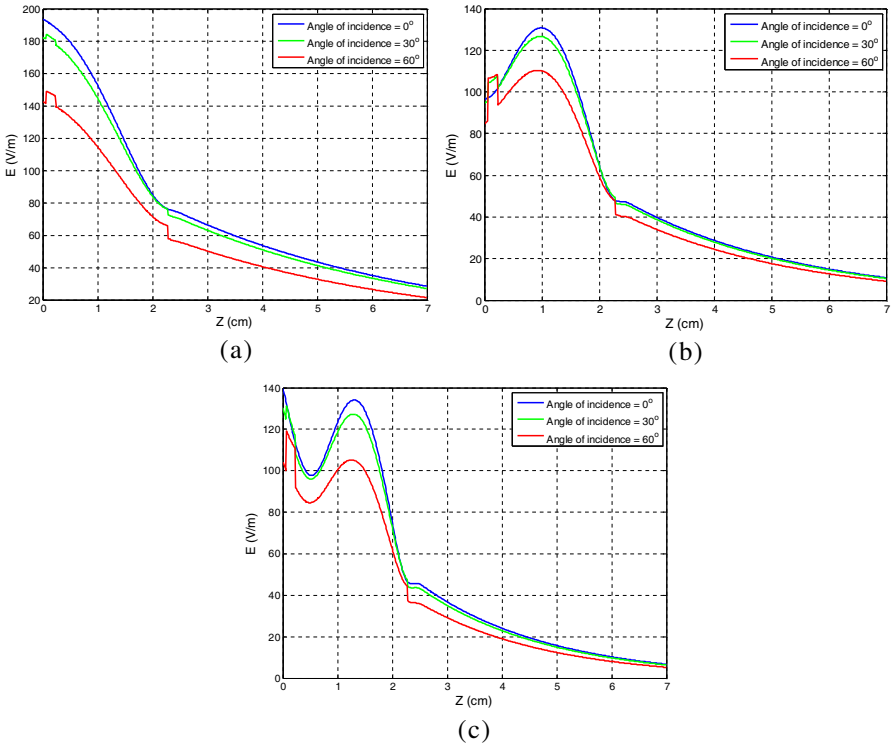

Figure 3. Induced total electric field intensity in the head model for parallel polarization ($E_{fo} = 300$ V/m) at (a) 900 MHz, (b) 1800 MHz, (c) 2.4 GHz.

interfaces between different layers. On the other hand, for parallel polarization, the electric field has two components; one of these two components is tangential to the interface while the other is not. So, the total electric field is not continuous across the interfaces for the parallel polarization case.

Once the field distribution is known, the SAR distribution in the different layers of the head model can be calculated. Figures 4 and 5 represent the SAR distributions for different angles of incidence at 900 MHz, 1800 MHz and 2.4 GHz for perpendicular and parallel polarizations, respectively. SAR distribution has its own shape at each frequency which is due to the fact that the electric properties of living tissues depend mainly on the frequency of the wave. Moreover, as the angle of incidence increases, the SAR values decrease. It is noted that the SAR peaks occur in the skin and CSF layers. The international accepted level for the SAR is 2 W/kg. For perpendicular polarization,

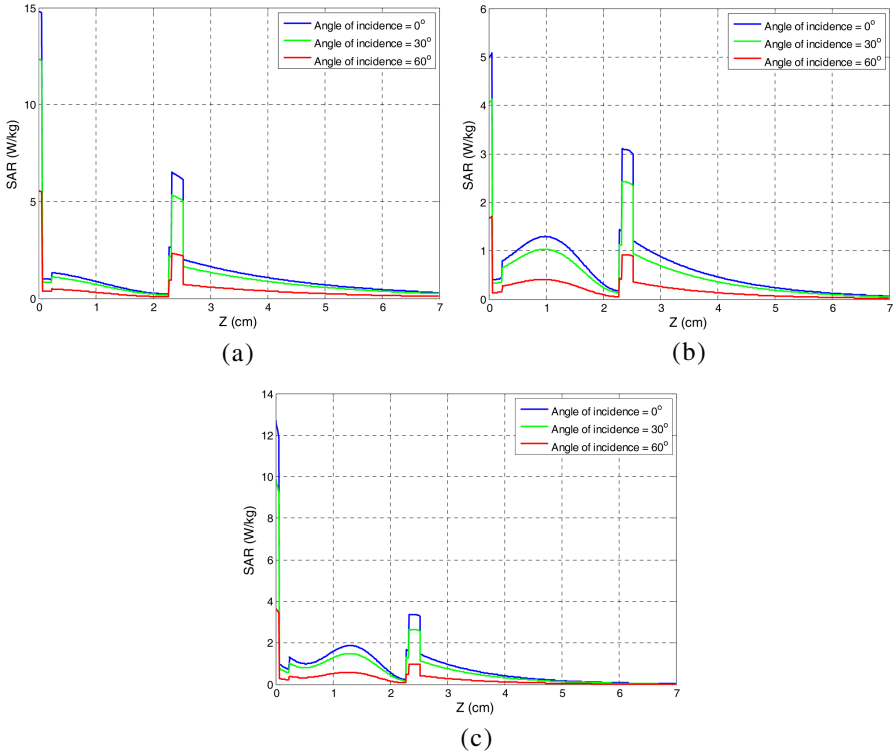

Figure 4. SAR distribution in the head model for perpendicular polarization at (a) 900 MHz, (b) 1800 MHz, (c) 2.4 GHz.

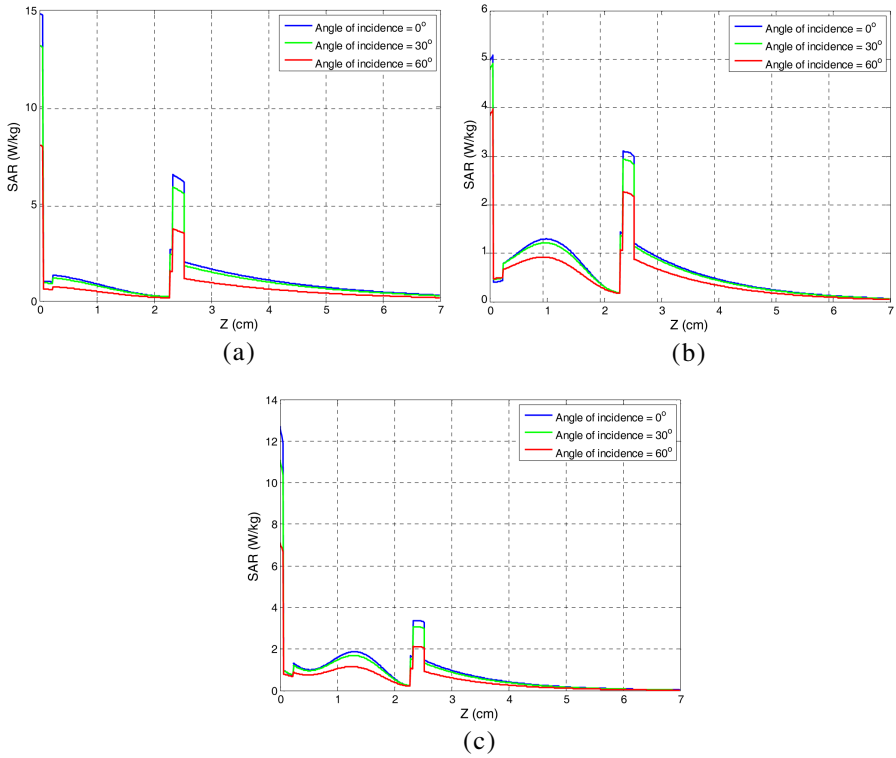

Figure 5. SAR distribution in the head model for parallel polarization at (a) 900 MHz, (b) 1800 MHz, (c) 2.4 GHz.

this value is exceeded in the CSF layer for the 0° (normal incidence) and 30° incidence angles, while it is exceeded in the skin layer for the three angles of incidence. Moreover, for parallel polarization, this value is exceeded in both the skin and CSF layers for the three angles of incidence as shown in Figure 5. It has been found that for perpendicular polarization, at 45° incidence angle, the SAR peak occurring in the CSF tissue will be less than the international limit. However, the SAR peak occurring in the skin tissue becomes less than the international limit at 71.5° angle of incidence. On the other hand, for parallel polarization, the peak of the SAR occurring in the CSF tissue becomes less than the international limit at an incidence angle of 65°; while the SAR peak occurring in the skin becomes less than the international limit at an angle of 78°.

Compared with the results obtained in [5] and [14], the obtained SAR values are very close to the FDTD simulation of other complicated

head models. In the literature, the cell resolutions used are inadequate to find the actual SAR value in very thin tissues and it is averaged or even neglected. This is the reason behind the fact that the obtained peak values in this work are higher than those found in [14].

The steady-state temperature computation provides information on the maximum temperature rise within the human head exposed to the RF fields from wireless applications. Figures 6 and 7 show the temperature-rise distribution at the frequencies of interest and for different angles of incidence for perpendicular and parallel polarizations, respectively.

It should be pointed out that even though the peak SAR occurs at the skin tissue, the peak temperature rise occurs within the internal bone tissue rather than the skin tissue. This is due to the fact that the temperature distribution is affected by the environment, imposed boundary conditions, thermal conductivity and blood perfusion rate

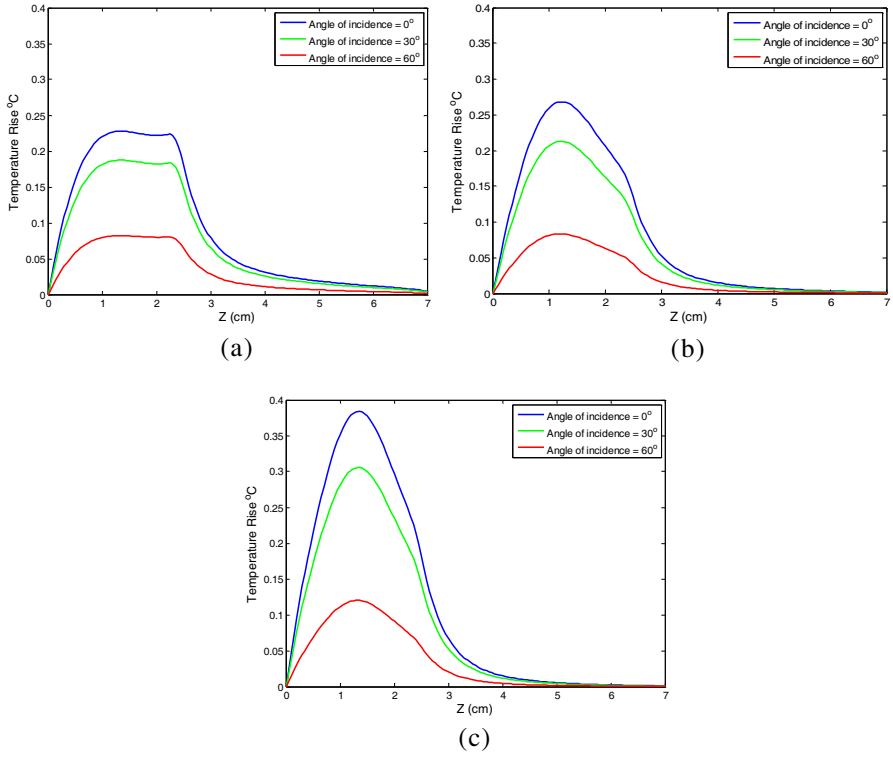

Figure 6. The steady state temperature-rise distribution model for perpendicular polarization at (a) 900 MHz, (b) 1800 MHz, (c) 2.4 GHz.

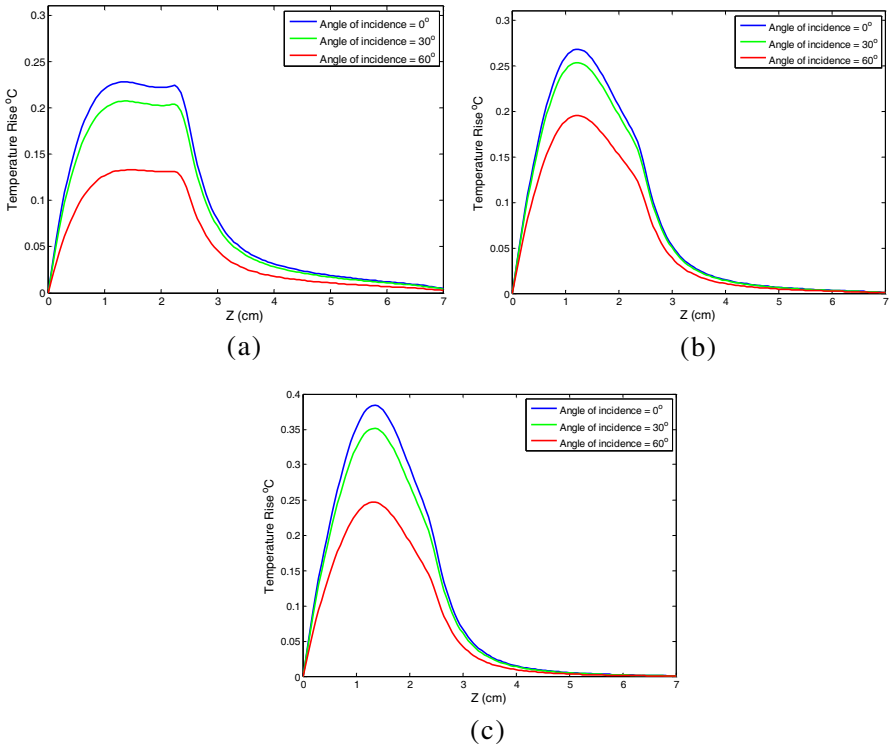

Figure 7. The steady state temperature-rise distribution model for parallel polarization at (a) 900 MHz, (b) 1800 MHz, (c) 2.4 GHz.

inside the living tissues. Moreover, bone has a low blood perfusion rate along with a high thermal conductivity. This means that the dissipated power by the skull is not lost by the blood flow like the skin.

It is found that the peak temperature rise increases exponentially over the first 9–10 minutes, then the rate of temperature rise slows down. The steady state is reached after about 25 minutes of exposure. Our results agree with those presented in [13] and [15].

It is clear from Figures 6 and 7 that as the angle of incidence increases, the temperature elevation decreases. In order to compare the temperature elevation at the different frequencies, Tables 4 and 5 show the peak temperature elevation at different frequencies and angles of incidence at the beginning of the brain tissue and in the skull for perpendicular and parallel polarizations, respectively.

The highest temperature elevation is 0.384°C which occurs in the skull at 2.4 GHz with a zero angle of incidence (i.e., normal incidence

Table 4. Peak temperature elevation at different frequencies and incidence angles (perpendicular polarization).

Angle of	Skull Tissue			Brain Tissue		
incidence	900 MHz	1800 MHz	2.4 GHz	900 MHz	1800 MHz	2.4 GHz
0°	0.227	0.268	0.384	0.14	0.095	0.13
30°	0.186	0.21	0.3	0.11	0.08	0.10
60°	0.082	0.087	0.12	0.05	0.03	0.04

Table 5. Peak temperature elevation at different frequencies and incidence angles (parallel polarization).

Angle of	Skull Tissue			Brain Tissue		
incidence	900 MHz	1800 MHz	2.4 GHz	900 MHz	1800 MHz	2.4 GHz
0°	0.227	0.268	0.384	0.14	0.095	0.13
30°	0.20	0.253	0.35	0.12	0.09	0.12
60°	0.13	0.195	0.24	0.08	0.074	0.085

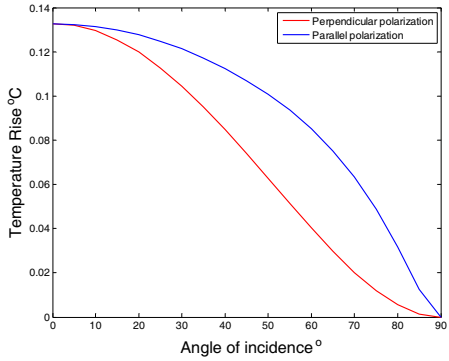

Figure 8. Peak temperature rise in the brain tissue at different angles of incidence at 2.4 GHz for both polarizations.

case). Moreover, it is known that the brain has the largest blood-flow rate in the head, so that temperature rise slows down rapidly. However, since the normal active heat transfer is very effective in regulating the temperature in the brain, a temperature rise up to 3.5°C in the brain is harmless and does not cause any physiological damage [13]. Figure 8 compares the peak temperature elevation in the brain tissue versus the angle of incidence for both polarizations.

It is clear that as the angle of incidence increases, temperature elevation decreases faster in the case of perpendicular polarization as

compared to the case of parallel polarization. This may be due to the fact that (at a specific incidence angle) a higher wave reflection occurs in the perpendicular polarization case as compared to the parallel polarization case.

4. CONCLUSIONS

SAR distribution and temperature increase have been evaluated in a head model exposed to oblique incident plane wave radiated from cellular phones and WLAN antennas for the two types of polarization. As the angle of incidence increases, temperature elevation decreases faster in the case of perpendicular polarization compared to the parallel polarization case. Moreover, the obtained results confirm the importance of performing a thermal analysis together with the dosimetric one. SAR levels in the tissues are less than the safety limit recommendations, except in the skin and CSF tissues. However, it is found that the induced temperature elevation in the head model, in all of the examined conditions, never exceeds 0.4°C. This value is well below the threshold for the induction of adverse thermal effects to the neurons. Even though the used head model was simple, the obtained results were very close to those presented in the literature using more sophisticated models. This model enabled us to make simulations with very small cell size, and thus, figuring out the effect of thin layers on the SAR distribution was possible in a small simulation time.

REFERENCES

1. IEEE, "IEEE standard for safety levels with respect to human exposure to radio frequency electromagnetic fields, 3 kHz to 300 GHz," *IEEE Std C95.1-2005*, 2005.
2. International Commission on Non-ionizing Radiation Protection (ICNIRP), "Guidelines for limiting exposure to time-varying electric, magnetic, and electromagnetic fields (up to 300 GHz)," Health Physics Society, 1998.
3. Riu, P. J. and K. R. Foster, "Heating of tissue by near-field exposure to a dipole: A model analysis," *IEEE Transaction on Biomedical Engineering*, Vol. 46, No. 8, 911–917, 1999.
4. Khalatbari, S., D. Sardari, A. A. Mirzaee, and H. A. Sadafi, "Calculating SAR in two models of the human head exposed to mobile phones radiations at 900 and 1800 MHz," *PIERS Online*, Vol. 2, No. 1, 104–109, 2006.
5. Bernardi, P., M. Cavagnaro, S. Pisa, and E. Piuzzi, "Power

absorption and temperature elevations induced in the human head by a dual-band monopole-helix antenna phone," *IEEE Trans. Microwave Theory Tech.*, Vol. 49, No. 12, 2539–2546, 2001.

6. Abdalla, A. and A. Teoh, "A multi layered model of human head irradiated by electromagnetic plane wave of 100 MHz–300 GHz," *Int. J. Sci. Res.*, Vol. 15, 1–7, 2005.
7. Andreuccetti, D., R. Fossi, and C. Petrucci, "Dielectric properties of the body tissues," last retrieved on Dec. 2009, http://niremf.ifac.cnr.it/tissprop/htmlclie/htmlclie.htm.
8. Furse, C., D. A. Christensen, and C. H. Durney, *Basic Introduction to Bioelectromagnetics*, 2nd edition, CRC Press, 2009.
9. Omar, A. A., Q. M. Bashayreh, and A. M. Al-Shamali, "Investigation of the effect of obliquely incident plane wave on a human head at 900 MHz and 1800 MHz," *Int. J. of RF and Microwave CAE*, Vol. 20, No. 2, 133–140, March 2010.
10. Moneda, A. P., M. P. Ioannidou, and D. P. Chrissoulidis, "Radiowave exposure of the human head: Analytical study based on a versatile eccentric spheres model including a brain core and pair of eyeballs," *IEEE Transactions on Biomedical Engineering*, Vol. 50, No. 6, 667–676, June 2003.
11. Pennes, H. H., "Analysis of tissue and arterial blood temperatures in resting forearm," *J. Applied Physiology*, Vol. 1, No. 2, 93–122, August 1948.
12. Hirata, A., K. Shirai, and O. Fujiwara, "On averaging mass of SAR correlating with temperature elevation due to a dipole antenna," *Progress In Electromagnetics Research*, Vol. 84, 221–237, 2008.
13. Wang, J. and O. Fujiwara, "FDTD computation of temperature rise in the human head for portable telephones," *IEEE Transaction on Microwave Theory Technology*, Vol. 47, 1528–1534, 1999.
14. Gasmelseed, A. and J. Yunus, "Specific absorption rate (SAR) on the human head as function of orientation of plane wave radiation: FDTD-based analysis," *Second Asia International Conference on Modelling & Simulation*, 959–962, 2008.
15. Chen, H.-Y. and H.-P. Yang, "Temperature increase in human heads due to different models of cellular phones," *Electromagnetics*, Vol. 26, 439–459, 2006.